Searching for Core-Collapse Supernova neutrinos at KM3NeT

Isabel Goos[a,*] **, Sonia El Hedri, Corinne Donzaud, Meriem Bendahman, Vladimir Kulikovskiy, Godefroy Vannoye and Damien Dornic on behalf of the KM3NeT Collaboration**

[a]*Particles Group, Astroparticle and Cosmology Laboratory (APC)*
10 Rue Alice Domon et Léonie Duquet, 75013 Paris, France

E-mail: goos@apc.in2p3.fr, elhedri@apc.in2p3.fr

The discovery of 25 neutrinos coming from the SN1987A core-collapse supernova (CCSN) by the Super-Kamiokande, IMB and Baksan experiments marked the beginning of neutrino astronomy. A new observation of supernova neutrinos with current or upcoming experiments could provide key insight into the underlying mechanism of CCSNe, which is currently poorly understood. Due to the low interaction rate of neutrinos, experiments are however only sensitive to close-by supernovae. Since these events are quite rare, it is crucial to optimize the detection channels of all available experiments. In this contribution, a study of the backgrounds for CCSN searches at the KM3NeT neutrino telescope, currently under construction and taking data in the Mediterranean Sea, is presented. Using new dedicated observables, signatures from radioactive decays and atmospheric muons are modelled, and these results are compared to data to assess the quality of the modelling of the detector response to supernova neutrinos. Finally, based on these results, an improvement of 23% in KM3NeT's distance horizon to a CCSN is presented.

*Speaker

1. Introduction

Core-Collapse supernovae (CCSNe) are the end of life of heavy stars (8M$_\odot$ and above), whose core collapses in a fraction of a second, often leading to an extremely powerful explosion whose mechanism is not yet completely understood. The detection of 25 neutrinos from supernova 1987A has demonstrated that CCSNe are associated with an extremely powerful neutrino emission, which could crucially affect the dynamics of this explosion. If another CCSN occurs in or near our Galaxy, the detection of the resulting $O(10)$ MeV neutrino burst would provide invaluable information on the CCSN mechanism and neutrino properties. Moreover, this burst could be intense enough to be visible at experiments targeting higher-energy neutrinos, such as KM3NeT.

KM3NeT [1] is a cubic-kilometer neutrino observatory currently under construction in the Mediterranean Sea. It is based on the detection of Cherenkov light induced by product particles of neutrino interactions in seawater. This light is detected by Digital Optical Modules (DOMs) arranged in groups of 18 along vertical *detection lines*. KM3NeT is composed of two detectors: ORCA, a densely instrumented 115-line array aimed at the characterization of $O(10)$ GeV neutrino oscillations, and ARCA, a kilometer-cube detector with two 115-line arrays aimed at the detection of TeV to PeV astrophysical neutrinos. To date, 21 lines have been installed at ARCA and 18 at ORCA. By the end of the year, ARCA will have 29 lines and ORCA 24 lines. In this study, these near-future ARCA29 and ORCA24 configurations are therefore considered.

KM3NeT's current CCSN search strategy [2] makes the detector's final configuration sensitive to 96% of Galactic CCSNe by leveraging its unique DOM structure. The present study shows how to further exploit this structure to improve KM3NeT's low-energy detection potential.

2. Low-energy neutrino signatures at KM3NeT

Interactions of $O(10)$ MeV neutrinos, such as CCSN neutrinos, will generally activate at most one DOM and hence are below KM3NeT's reconstruction threshold. If their single-DOM signatures were not resolved, low-energy neutrinos would be indistinguishable from KM3NeT's main backgrounds: bioluminescence, ambient radioactivity, and atmospheric muons as well as muons from neutrino interactions. However, each KM3NeT DOM is composed of 31 small photomultipliers (PMTs), grouped into a sphere of 21.6 cm radius, as shown in Figure 1, left [3]. This small but dense PMT array can be used to characterize low-energy neutrino signatures.

In particular, KM3NeT's current CCSN analysis uses the *multiplicity*, defined as the number of PMT hits in a DOM within a 10 ns window, to distinguish CCSN neutrinos from ambient backgrounds [2, 4]. An example of a multiplicity 4 signature is shown in Figure 1, left. The multiplicity distribution for a 6 hour period of ORCA6 is shown in Figure 1, right. Simulations show that the low multiplicity region up to a value of 7 is dominated by radioactive decays in seawater, while muons dominate the background at values above 7. This contribution presents a proposal for improving KM3NeT's sensitivity to low-energy neutrinos by considering not only the multiplicity of a single-DOM signal but also other single-DOM observables, such as the signal's position on the DOM, and the time and space correlations between activated PMTs.

After considering a wide array of possible single-DOM observables, four weakly-correlated quantities are selected. $\cos\theta$ is the zenith angle of the average direction of the activated PMTs and

thus indicates the position of the signal on the DOM. The spatial concentration of activated PMTs is captured by the $|R|$ observable, which is the magnitude of the average direction of activated PMTs. The last two observables considered are the total time over threshold (ToT), which reflects the intensity of the signal, and Δt, which is the mean time difference between the first hit of a coincidence and the rest of the hits and indicates thus the temporal spread of the signal. The distributions of these four observables for simulated events at the ORCA detector with a 6-line configuration are shown in Figure 2, selecting events with multiplicity 8 that are not associated with KM3NeT high-energy triggers. GEANT4-based simulations of the two dominant KM3NeT backgrounds for this multiplicity are also shown: radioactivity, notably from ^{40}K in the seawater, and muons. The quality of these simulations is validated by comparing the shapes of the resulting distributions to data. These shapes are found to be similar between data and simulations. The remaining differences will be accounted for in subsequent analyses as systematic uncertainties.

The shapes of the $|R|$, $\cos\theta$, and Δt distributions differ significantly between radioactivity and muon backgrounds, showing the excellent discriminating potential of these observables. In particular, these new quantities capture essential differences between radioactivity and muons, which do not necessarily translate into multiplicity differences, as shown in the $\cos\theta$ and $|R|$ distributions in Figure 2. Long downward-going muon tracks leave spread-out signatures (low $|R|$), mostly on the upper half of the DOMs (large $\cos\theta$). Conversely, low-energy radioactivity signals occur more often near the bottom of the DOM (low $\cos\theta$), which is more instrumented, and are emitted close to the DOM, thus activating small groups of close-by PMTs (large $|R|$). In addition to these observables, for higher multiplicities where muon backgrounds dominate, the total ToT also becomes an essential background characterization tool.

In the following section, the single-DOM observables presented above are incorporated into a multivariate analysis, in order to improve KM3NeT's sensitivity to CCSN neutrinos.
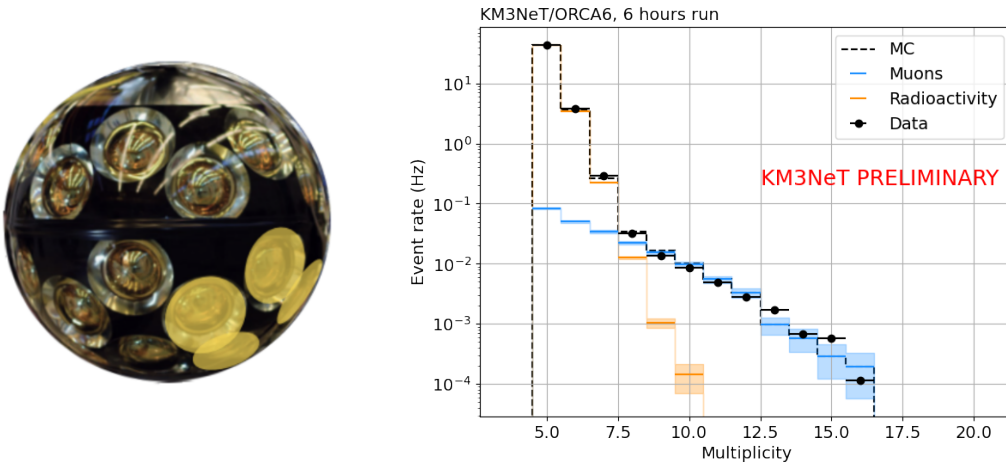
Figure 1: Left: image of a DOM with 4 out of the 31 PMTs highlighted to show an example of a multiplicity 4 low-energy neutrino signature. Right: Multiplicity distribution for a 6 hour period of ORCA6 (full black) compared to simulations. Simulated muons are shown in blue, simulated radioactive decays in orange and the total simulated background in dashed black.

3.　Searching for CCSN neutrinos

Neutrinos emitted by a Galactic CCSN could leave signatures in individual KM3NeT DOMs, as discussed in the previous section. If the neutrino burst is intense enough, these signatures could register as a rise of the number of recorded single-DOM events at ORCA and ARCA, lasting for about 0.5 s. To identify this rise, an online analysis system [4] processes ORCA and ARCA data in realtime, selects suitable CCSN candidates among single-DOM events based on their multiplicity, and evaluates the expected background level. This background is dependent of the number of active PMTs, and its characterization is described in PoS(2023)1223. The number of candidates in a sliding 0.5 s window is then computed and, if the false alarm rate is less than 0.125 per day, a CCSN trigger is issued and an alert is sent to the Supernova Early Warning System (SNEWS, [5]). This
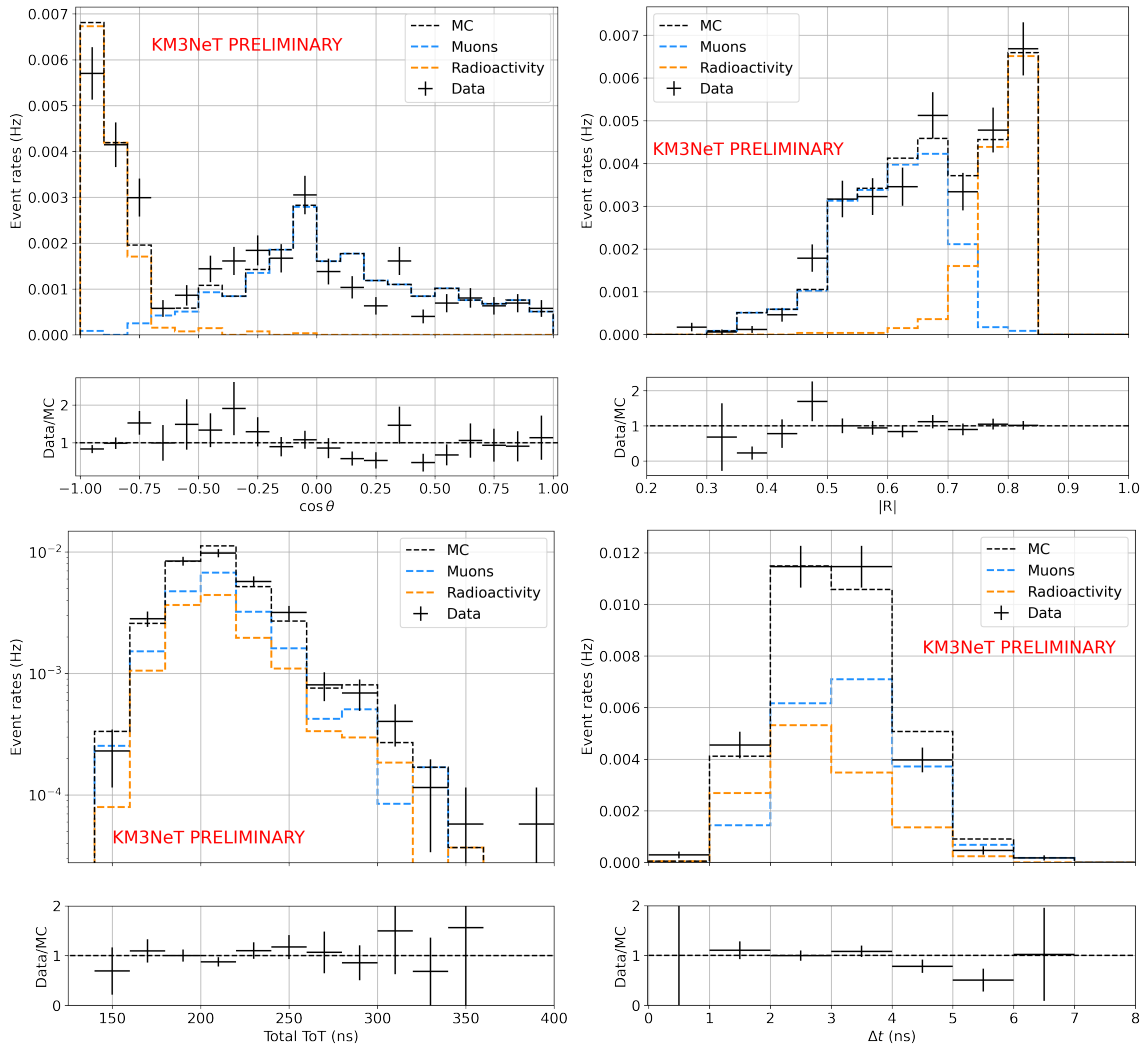

Figure 2: Distributions of the most relevant new single-DOM observables for ORCA6 data compared to simulations: $\cos\theta$ (top left), $|R|$ (top right), total ToT (bottom left) and Δt (bottom right). ORCA6 data is shown with full black lines, while MC is shown with dashed black lines (muons in blue and radioactivity in orange).

contribution focuses on improving the CCSN candidate selection to increase the sensitivity of this CCSN trigger.

The present analysis relies on two event selection steps. First, a muon veto based on current high-energy KM3NeT triggers is applied to reduce the muon background. The expected number of events in ORCA24 and ARCA29 after applying the muon veto and as a function of the multiplicity is shown in Figure 3, left. The muon veto is more efficient for ORCA than ARCA since the ORCA array is denser. The simulated signal from a CCSN expected at ORCA24 & ARCA29 for a distance of 8 kpc is also shown in this figure for different progenitor masses. These simulations are based on the models from [6–8] for the progenitors of $11 M_\odot$, $27 M_\odot$ and $40 M_\odot$, respectively. The total CCSN rate expected at a water Cherenkov detector is then computed using the SNEWPY software [9] and the result is rescaled to the size of ORCA24 & ARCA29. As can be seen in Figure 3, the signal can be clearly identified above the background contribution at intermediate multiplicity values.

Second, a method to select signal-like single-DOM events is developed, making use of the observables described in Section 2. For this purpose, Boosted Decision Trees (BDTs) are used. BDTs are a machine learning technique which is used in this analysis to assess how signal-like an event is, based on the values of the single-DOM observables. Since the background and signal distributions are different for different multiplicities, one BDT is trained for each multiplicity between 5 and 9 (below 5 the background is too high and above 9 the statistics of our data and simulation samples becomes too low). In addition, since the muon veto affects the ORCA and ARCA
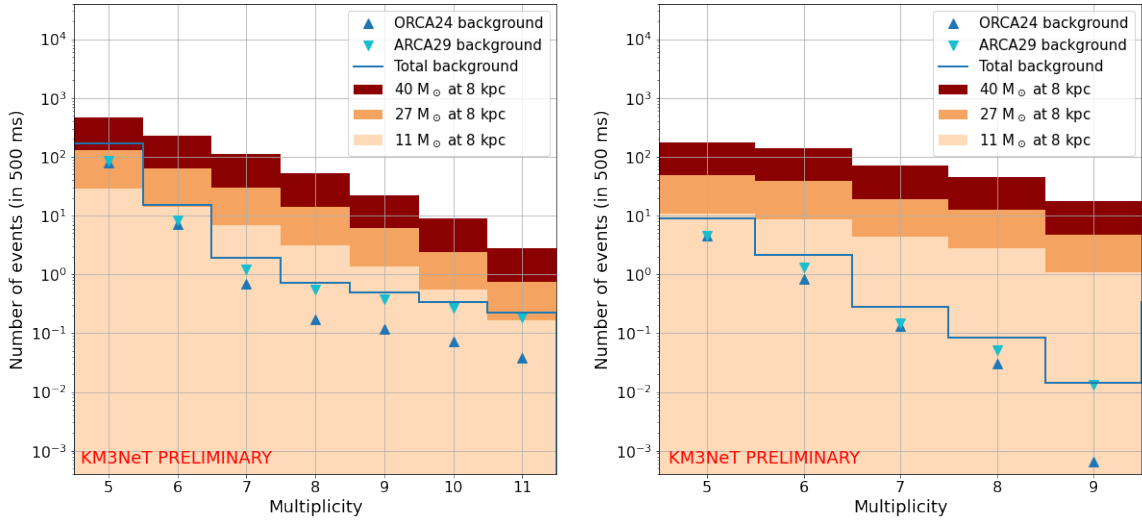
Figure 3: Expected number of events in ORCA24 and ARCA29 as a function of the multiplicity before (left) and after (right) applying the BDT cuts (where only the multiplicities for which a BDT cut is applied are displayed). In both cases, the muon veto is applied. The background is shown separately for ORCA24 (light blue markers) and ARCA29 (dark blue markers); the sum of the two is shown with a blue line. The signal of a CCSN at a distance of 8 kpc is represented with coloured bars in orange shades for different models: light for $11 M_\odot$, intermediate for $27 M_\odot$, and dark for $40 M_\odot$.

backgrounds differently, BDTs for ORCA and ARCA are trained using ORCA6 data (livetime of 463 h) and ARCA8 data (livetime of 293 h) as backgrounds, respectively. During the training process, the $11M_\odot$ model is used for the signal, since it is the most probable supernova scenario considered here.

BDTs are trained using different subsets of the single-DOM observables described in Section 2 as input features. The distribution of the discriminant for a BDT trained on ORCA6 events and restricted to multiplicity 8 is shown in Figure 4. The jagged shape of the curves is due to the discrete segmentation of the DOM. For each multiplicity, the BDT selection is then optimized by minimizing the number of signal events needed for a 5σ discovery, using the Rolke method [10]. This is a frequentist method that takes uncertainties in the background and event selection efficiency into account. In this analysis, background rates are estimated using large data samples collected with the most recent detector configurations, as well as GEANT4-based simulations for the CCSN signal. Systematic uncertainties associated with the signal simulation are modelled using the relative discrepancies between the data and background simulations introduced in Section 2. Uncertainties on the DOMs' efficiencies and the number of activated PMTs are taken to be of 11%, following the estimates from [2].

Applying the optimal BDT cuts in addition to the muon veto to the background and simulated signal distributions leads to the distributions shown in Figure 3, right. With this procedure, a considerable reduction of the background with respect to the signal is achieved. In particular, after the cut on the BDT score, the signal at multiplicity 6 is now above the background even for the lightest progenitor.

4. Distance horizons

After applying the muon veto and the optimal BDT cuts to background and signal events, the optimal multiplicity range is computed for the combined detector ORCA24 & ARCA29, scanning
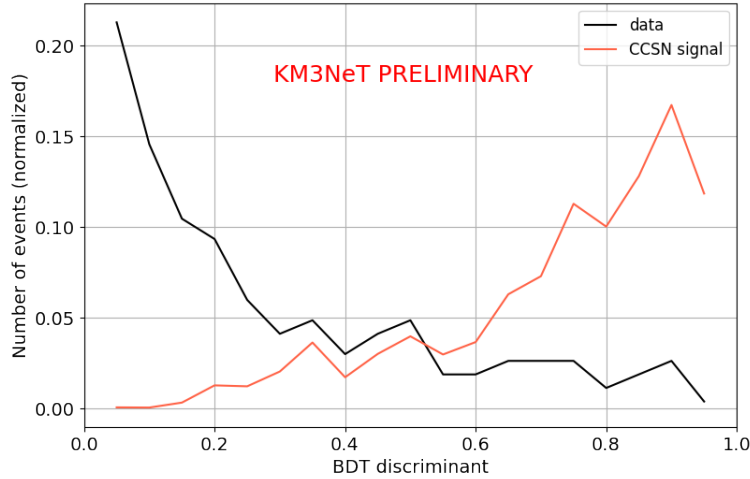

Figure 4: BDT discriminant distribution for a BDT trained on ORCA6 data, using $|R|$, $\cos\theta$ and the total ToT as input features, for events with multiplicity 8. The jagged shape of the curves is due to the discrete segmentation of the DOM.

multiplicities from 5 to 11 and again minimizing the number of signal events corresponding to a 5σ discovery. The 5σ distance horizon for the most conservative case of an $11M_\odot$ progenitor is shown in Figure 5, for all considered multiplicity ranges, before (left) and after (right) applying the BDT cuts. The best horizon without applying BDT cuts is at 8.1 kpc, selecting events in the multiplicity range 6-11. The use of BDT cuts leads to a 23% increase of this horizon, up to 10.0 kpc, using the multiplicity range 6-9. Hence, for the low-emission CCSN model considered, the use of single-DOM observables makes it possible for current detectors to probe a significant fraction of the Galactic bulge. In the cases of the $27M_\odot$ and $40M_\odot$ models, the 5σ distance horizons making use of the BDT cuts are at 21.1 kpc and 40.4 kpc, respectively.

It is also instructive to compute the sensitivity (in units of sigma) to a CCSN signal as a function of the distance from it. The result is shown in Figure 6 for the three progenitors considered and using the combined ORCA24 & ARCA29 detector and the optimal multiplicity range. The distance to Betelgeuse, which has a mass of close to $11M_\odot$, is also displayed as a reference, since it is a good candidate for the next Galactic supernova [11]. For this scenario, the detection of associated neutrinos would be certain. With the upcoming detector configuration considered, the analysis proposed here can reach the Galactic Center and, for a sufficiently heavy progenitor, a CCSN close to the most distant Milky Way edge could be detected.

5. Conclusions

The design of the DOMs at KM3NeT makes it possible to detect a CCSN signal despite the fact that CCSN neutrinos have energies below the detector's energy threshold. Here, a thorough study of single-DOM observables, which capture different characteristics of a MeV-scale signal, is performed. BDTs are used to discriminate signal from background events. With this method, KM3NeT's distance horizon is increased by 23%. With the upcoming ORCA24 and ARCA29
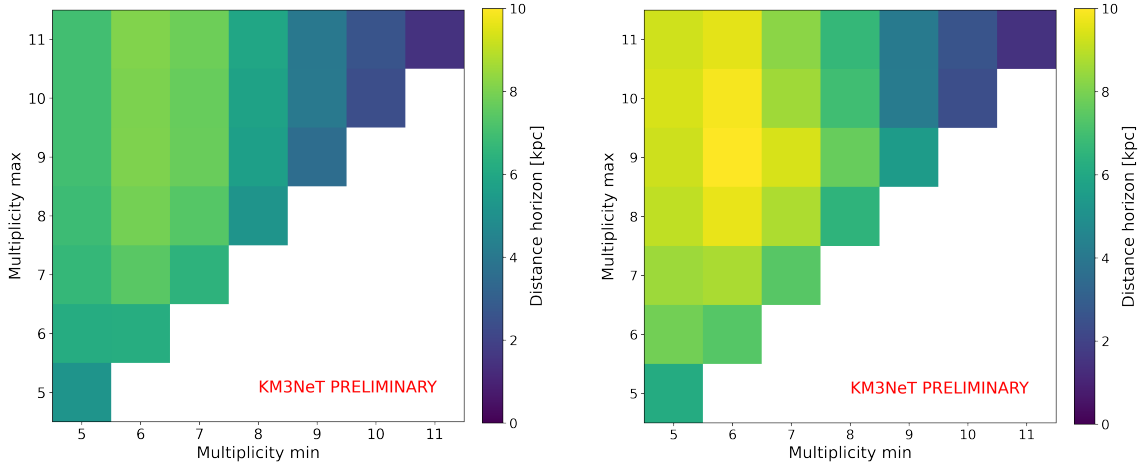
Figure 5: Distance horizons at 5σ obtained by selecting different multiplicity ranges, without BDT cuts (left) and with the optimal BDT cuts (right). The horizons for these two scenarios are of 8.1 kpc and 10.0 kpc, respectively.
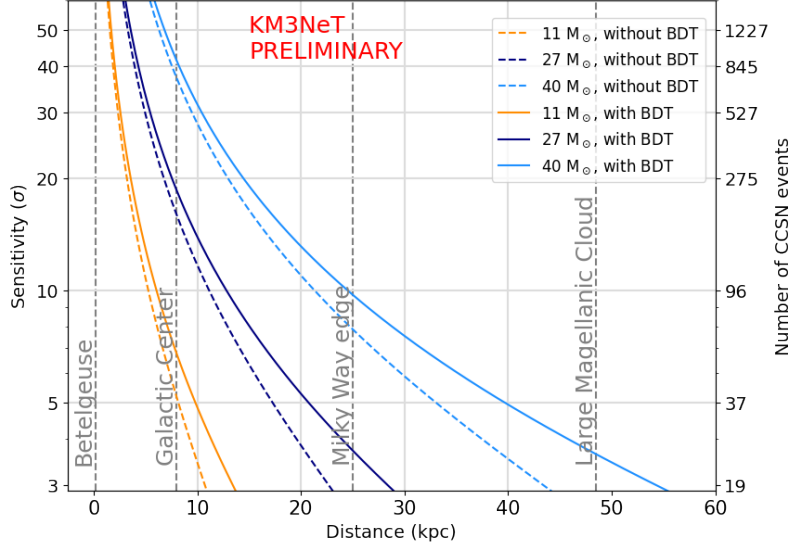
Figure 6: KM3NeT detection sensitivity as a function of the distance from the CCSN for the three progenitors considered: $11M_\odot$ (orange), $27M_\odot$ (dark blue) and $40M_\odot$ (light blue).

detector configurations it will thus be possible to probe a significant fraction of the Galactic bulge, even for the case of a light progenitor.

Acknowledgments

References

[1] S. Aiello *et al.* [KM3NeT], J. Phys. G: Nucl. Part. Phys. **43**, no.8, 084001 (2016).

[2] S. Aiello *et al.* [KM3NeT], Eur. Phys. J. C **81**, no.5, 445 (2021).

[3] S. Aiello *et al.* [KM3NeT], JINST **17**, no.7, P07038 (2022).

[4] S. Aiello *et al.* [KM3NeT], Eur. Phys. J. C **82**, no.4, 317 (2022).

[5] S. Al Kharusi *et al.*, New J. Phys. **23**, no.3, 031201 (2021).

[6] I. Tamborra *et al.*, Phys. Rev. Lett. **111**, no.12, 121104 (2013).

[7] I. Tamborra *et al.*, Phys. Rev. D **90**, no.4, 045032 (2014).

[8] L. Walk *et al.*, Phys. Rev. D **101**, no.12, 123013 (2020).

[9] A. Baxter *et al.*, Astrophys. J. **925**, no. 2, 107 (2022).

[10] W. A. Rolke *et al.*, Nucl. Instrum. Methods Phys. Res. A **551**, no.2-no.3, 493-503 (2005).

[11] H. Saio *et al.*, arXiv:2306.00287 [astro-ph.SR].